

Supporting Information

**A New Stable Luminescent Cd(II) Metal–Organic
Framework with Fluorescent Sensing and Selective Dye
Adsorption Properties**

Wen-Quan Tong, Wei-Ni Liu, Jian-Guo Cheng, Peng-Feng Zhang, Gao-peng Li, Lei Hou* and Yao-Yu Wang*

Key Laboratory of Synthetic and Natural Functional Molecule Chemistry of the Ministry of Education, Shaanxi Key Laboratory of Physico-Inorganic Chemistry, College of Chemistry and Materials Science, Northwest University, Xi'an, Shaanxi 710127, P. R. China. E-mail: wyaoyu@nwu.edu.cn. lhou2009@nwu.edu.cn.

Table S1. Selected bond lengths [Å] and angles [°] for complex **1**.

1			
Cd(1)-O(18)	2.172(10)	Cd(3)-O(3)#5	2.308(9)
Cd(1)-O(12)#1	2.223(9)	Cd(3)-O(7)	2.336(8)
Cd(1)-O(19)	2.290(13)	Cd(3)-O(9)	2.374(8)
Cd(1)-O(17)	2.321(13)	Cd(3)-O(4)#5	2.463(8)
Cd(1)-O(15)	2.336(9)	Cd(3)-O(8)	2.561(12)
Cd(1)-O(16)	2.388(9)	Cd(2)#3-O(5)	2.300(8)
Cd(2)-O(5)#2	2.299(8)	Cd(2)#2-O(13)	2.420(8)
Cd(2)-O(14)#3	2.324(8)	Cd(2)#2-O(14)	2.323(8)
Cd(2)-O(9)	2.409(8)	Cd(3)#5-O(11)	2.295(9)
Cd(2)-O(13)#3	2.421(8)	Cd(3)#4-O(4)	2.463(8)
Cd(2)-O(7)	2.426(9)	Cd(3)#4-O(3)	2.309(9)
Cd(2)-O(10)	2.427(9)	Cd(1)#6-O(12)	2.222(9)
Cd(3)-O(11)#4	2.295(9)	Cd(2)-N(1)#2	2.326(9)
N(1)-Cd(2)#3	2.326(9)	Cd(3)-N(4)#4	2.361(9)
O(18)-Cd(1)-O(19)	90.5(5)	N(4)-Cd(3)#5	2.361(9)
O(12)#1-Cd(1)-O(19)	83.9(6)	O(18)-Cd(1)-O(12)#1	131.8(4)
O(18)-Cd(1)-O(17)	94.1(5)	O(9)-Cd(2)-O(7)	76.9(3)
O(12)#1-Cd(1)-O(17)	88.4(5)	O(13)#3-Cd(2)-O(7)	90.4(3)
O(19)-Cd(1)-O(17)	172.3(5)	O(5)#2-Cd(2)-O(10)	130.8(3)
O(18)-Cd(1)-O(15)	80.3(3)	O(14)#3-Cd(2)-O(10)	78.8(3)
O(12)#1-Cd(1)-O(15)	146.8(3)	O(9)-Cd(2)-O(10)	53.3(3)
O(19)-Cd(1)-O(15)	88.5(5)	O(13)#3-Cd(2)-O(10)	131.3(3)
O(17)-Cd(1)-O(15)	98.4(4)	O(7)-Cd(2)-O(10)	102.5(3)
O(18)-Cd(1)-O(16)	136.6(4)	O(11)#4-Cd(3)-O(3)#5	144.6(3)

O(12)#1-Cd(1)-O(16)	90.8(3)	O(11)#4-Cd(3)-O(7)	92.3(3)
O(19)-Cd(1)-O(16)	85.8(4)	O(3)#5-Cd(3)-O(7)	122.9(3)
O(17)-Cd(1)-O(16)	95.0(5)	O(11)#4-Cd(3)-O(9)	94.0(3)
O(15)-Cd(1)-O(16)	56.3(3)	O(3)#5-Cd(3)-O(9)	96.0(3)
O(5)#2-Cd(2)-O(14)#3	147.8(3)	O(7)-Cd(3)-O(9)	79.3(3)
O(5)#2-Cd(2)-O(9)	89.2(3)	O(11)#4-Cd(3)-O(4)#5	91.3(3)
O(14)#3-Cd(2)-O(9)	122.5(3)	O(3)#5-Cd(3)-O(4)#5	54.9(3)
O(5)#2-Cd(2)-O(13)#3	92.6(3)	O(7)-Cd(3)-O(4)#5	169.3(3)
O(14)#3-Cd(2)-O(13)#3	55.2(3)	O(9)-Cd(3)-O(4)#5	90.3(3)
O(9)-Cd(2)-O(13)#3	167.3(3)	O(11)#4-Cd(3)-O(8)	134.4(4)
O(5)#2-Cd(2)-O(7)	97.2(3)	O(3)#5-Cd(3)-O(8)	75.1(3)
O(14)#3-Cd(2)-O(7)	86.0(3)	O(7)-Cd(3)-O(8)	52.3(3)
O(4)#5-Cd(3)-O(8)	129.2(3)	O(9)-Cd(3)-O(8)	104.3(4)

Symmetry transformations used to generate equivalent atoms: #1: $x+1/2, -y+1/2, z+1/2$; #2: $-x+3/2, y-1/2, -z+1/2$; #3: $-x+3/2, y+1/2, -z+1/2$; #4: $-x+1/2, y+1/2, -z+1/2$; #5: $-x+1/2, y-1/2, -z+1/2$; #6: $x-1/2, -y+1/2, z-1/2$.

Table S2 Standard Deviation (δ) calculation for the detection of Fe^{3+} for **1**.

Test	Fluorescence intensity (nm)
1	5408.519
2	5407.993
3	5407.633
4	5408.235
5	5408.432
6	5407.855
7	5407.944
8	5407.732
9	5408.439
10	5408.365
average	5408.115
Standard deviation (δ)	0.315

Table S3 Standard Deviation (δ) calculation for the detection of CrO_4^{2-} for **1**.

Test	Fluorescence intensity (nm)
1	5697.787
2	5696.832
3	5696.914
4	5696.798
5	5697.564
6	5697.643
7	5696.994
8	5697.441
9	5697.742
10	5697.698
average	5697.341
Standard deviation (δ)	0.408

Table S4 Standard Deviation (δ) calculation for the detection of $\text{Cr}_2\text{O}_7^{2-}$ for **1**.

Test	Fluorescence intensity (nm)
1	7681.412
2	7682.102
3	7682.094
4	7682.111
5	7681.564
6	7681.643
7	7682.204
8	7681.441
9	7681.742
10	7681.698
average	7681.801
Standard deviation (δ)	0.901

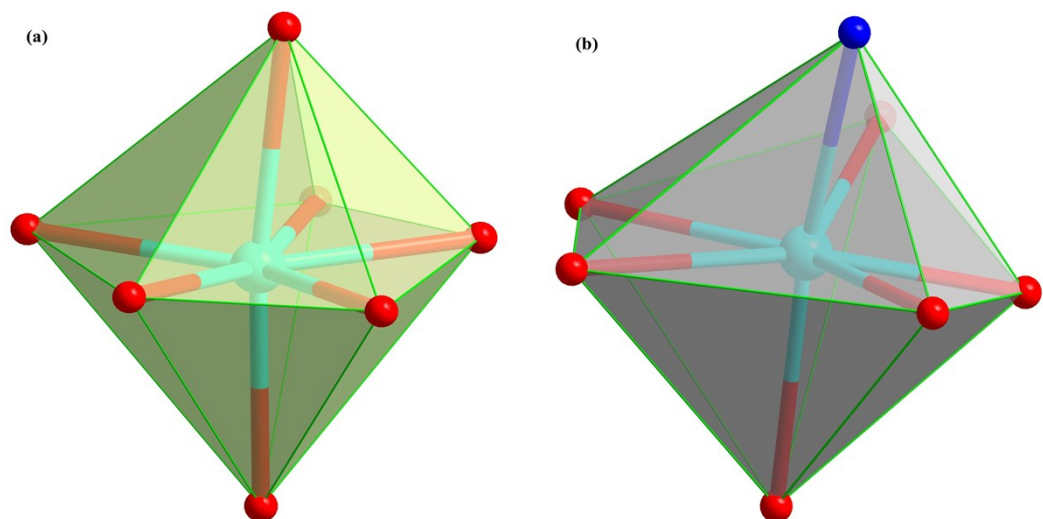


Fig. S1 Coordination arrangement of $\text{Cd}^{2+}1$ (a) and $\text{Cd}^{2+}2$, $\text{Cd}^{2+}3$ (b) ions could be described as a distorted pentagonal bipyramid.

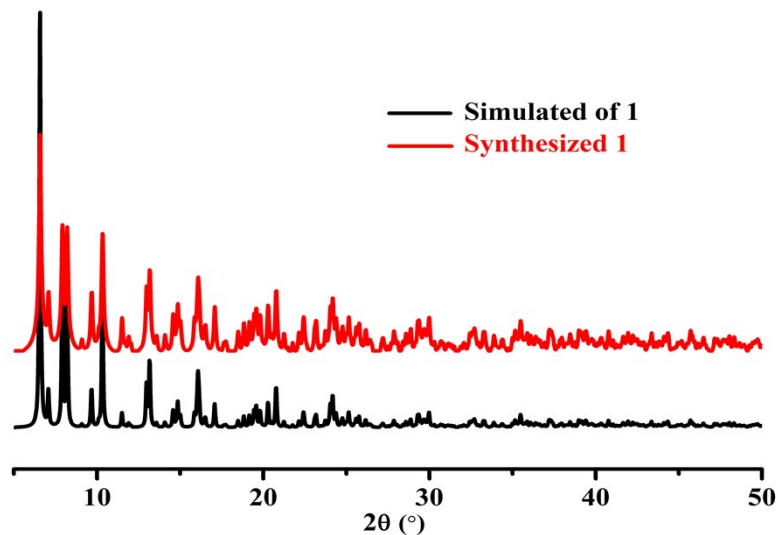


Fig. S2 PXRD patterns of complex **1** simulated from the X-ray single-crystal data and as-synthesized products.

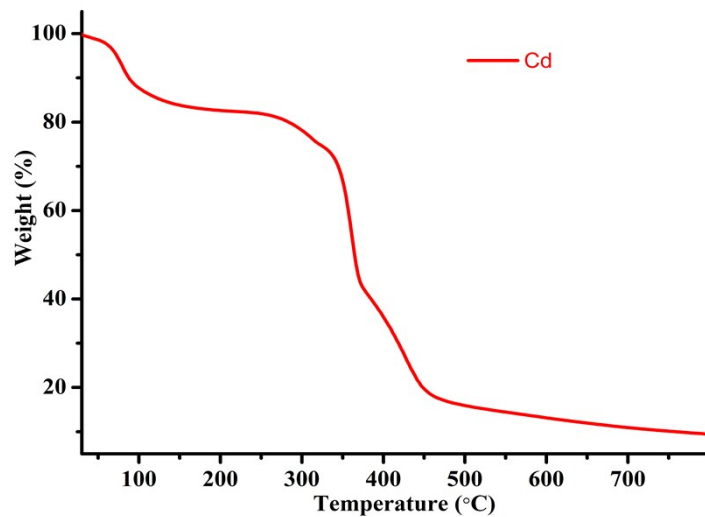


Fig. S3 The TGA curve of complex **1**.

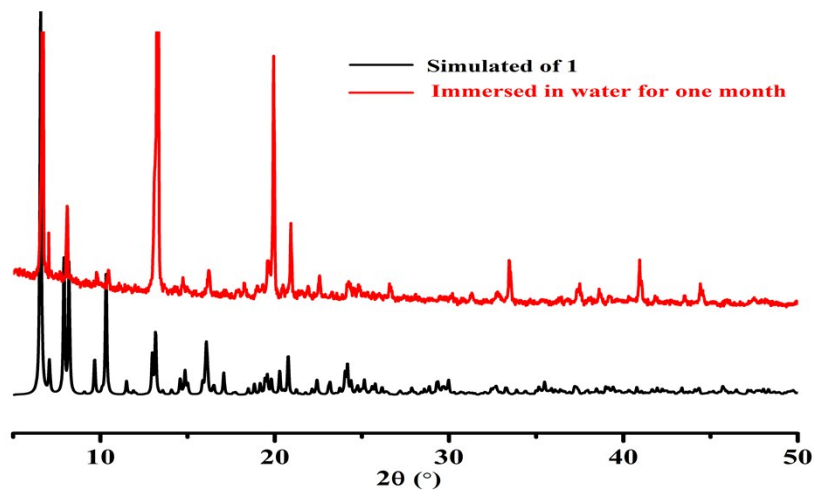


Fig. S4 PXRD patterns of **1** immersed in water at room temperature for one month.

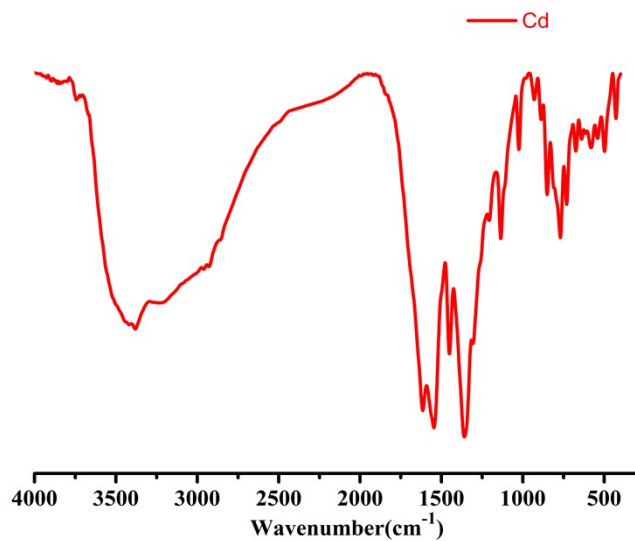
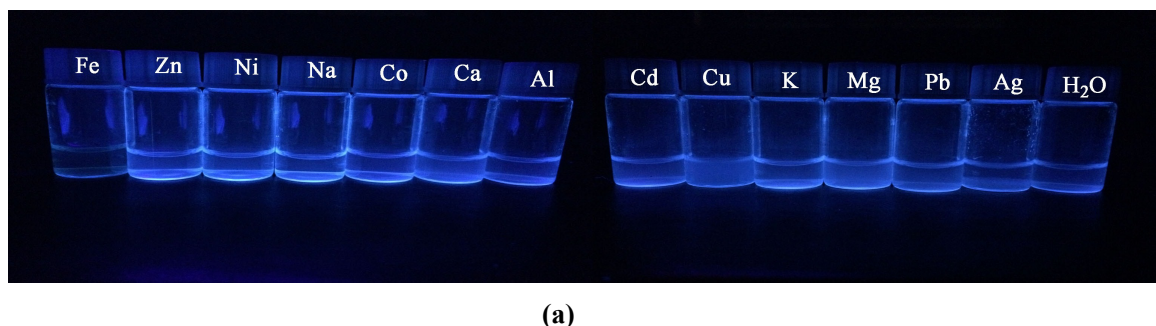
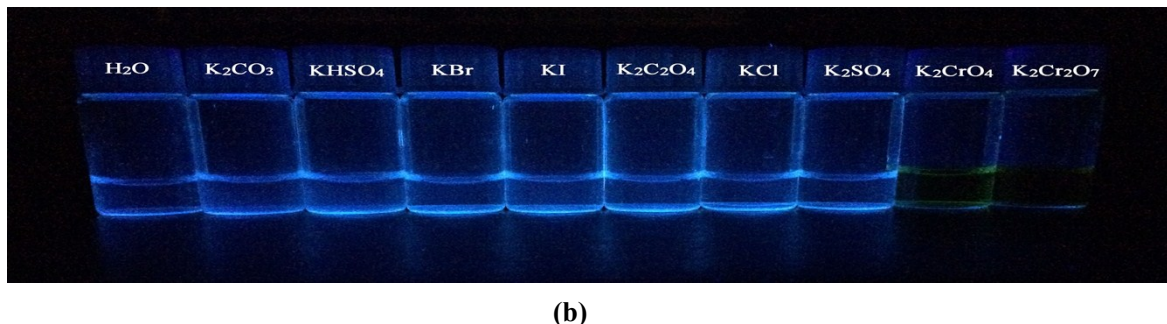


Fig. S5 The FT-IR spectra of complex **1**.

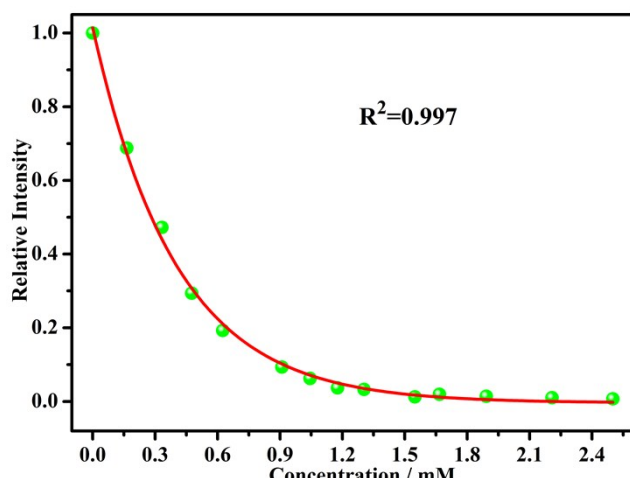


(a)

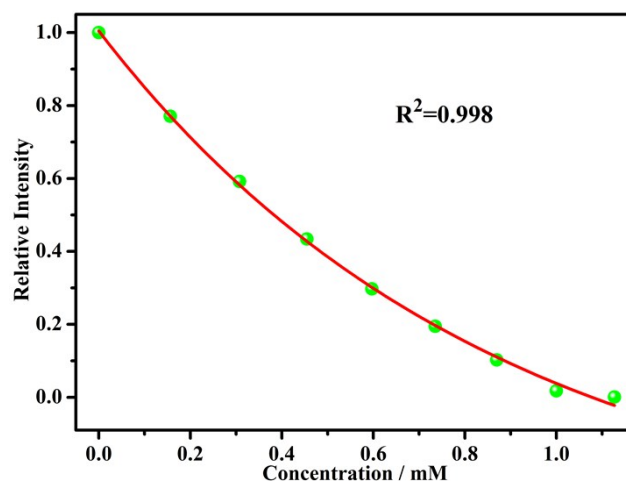


(b)

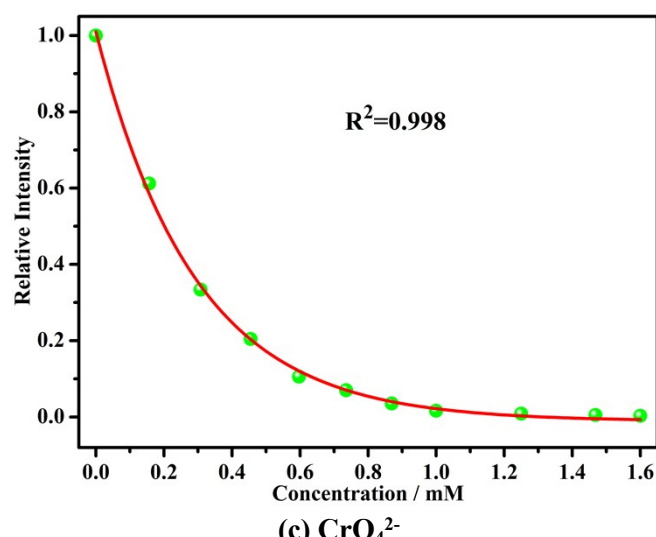
Fig. S6 (a) Pictures of different Mn⁺@**1** solutions (M = Cu²⁺, Mg²⁺, Al³⁺, Cd²⁺, Pb²⁺, Co²⁺, Ca²⁺, Zn²⁺, Na⁺, K⁺, Ni²⁺, Ag⁺ and Fe³⁺ respectively); (b) Pictures of different **1**@Aⁿ⁻ solutions (A = Cr₂O₇²⁻, CrO₄²⁻, HSO₄⁻, CO₃²⁻, Br⁻, Cl⁻, I⁻, C₂O₄²⁻ and SO₄²⁻ respectively).



(a) Fe^{3+}

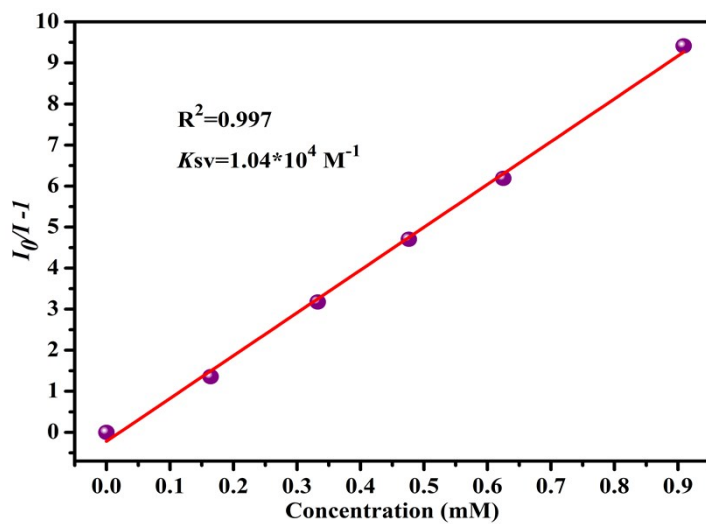


(b) $\text{Cr}_2\text{O}_7^{2-}$

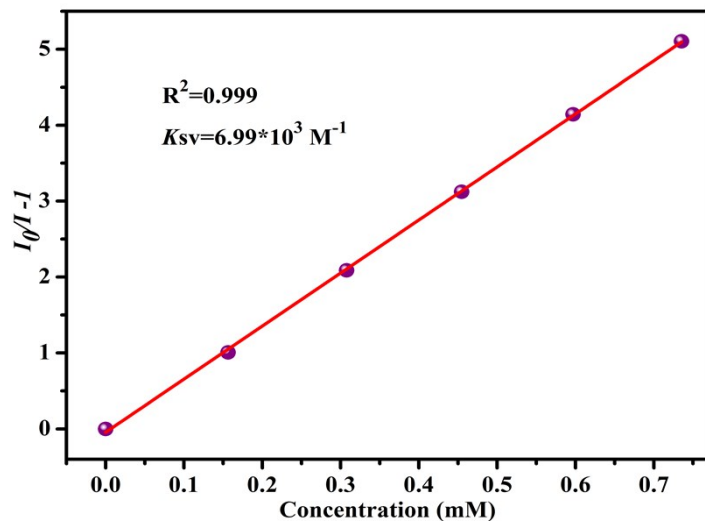


(c) CrO_4^{2-}

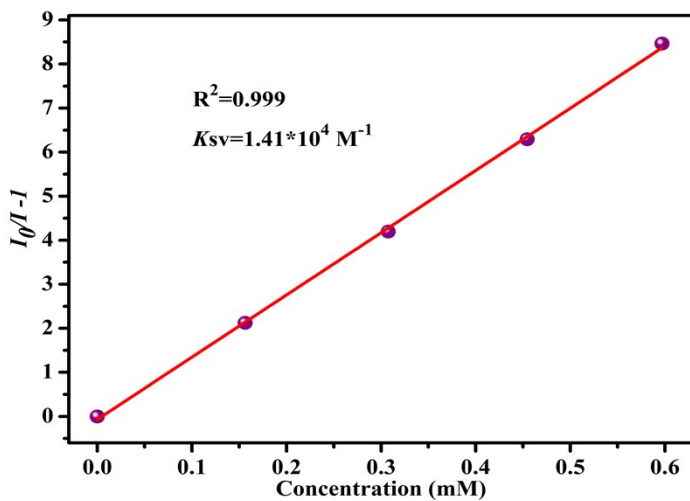
Figure S7 The linear correlation for the plot of I_0/I vs concentration of Fe^{3+} (a), $\text{Cr}_2\text{O}_7^{2-}$ (b) and CrO_4^{2-} (c) ions, respectively, in low concentration range.



(a) Fe^{3+}



(b) $\text{Cr}_2\text{O}_7^{2-}$



(c) CrO_4^{2-}

Fig. S8 Quenching efficiency defined by the Stern–Volmer relationship for Fe^{3+} , $\text{Cr}_2\text{O}_7^{2-}$ and CrO_4^{2-} ions.

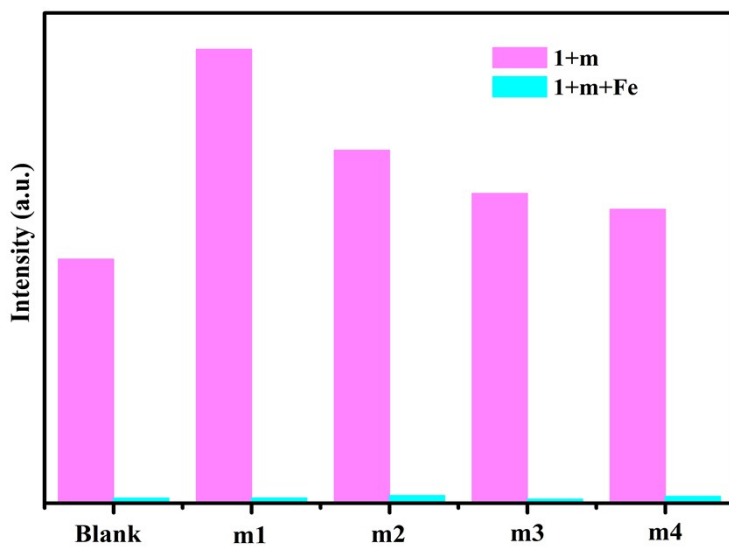


Fig. S9 Luminescence intensity at 406 nm of **1** dispersed in water with addition of different mixed ions (10^{-2} M) mixed solution added Fe^{3+} ions (10^{-2} M) (m1: $\text{Ag}^{2+}/\text{Pb}^{2+}$; m2: $\text{Cu}^{+}/\text{K}^{+}/\text{Mg}^{2+}$; m3: $\text{Al}^{3+}/\text{Cd}^{2+}/\text{Ca}^{2+}/\text{Co}^{2+}$; m4: $\text{Na}^{+}/\text{Ni}^{2+}/\text{Zn}^{2+}$).

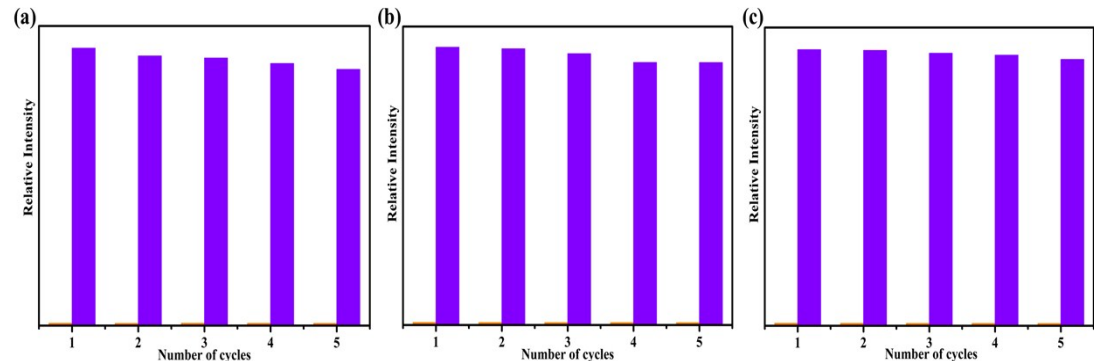


Fig. S10 Luminescent intensity at 406 nm of **1** after five recycles in Fe^{3+} , CrO_4^{2-} and $\text{Cr}_2\text{O}_7^{2-}$ solutions (10^{-2} M).

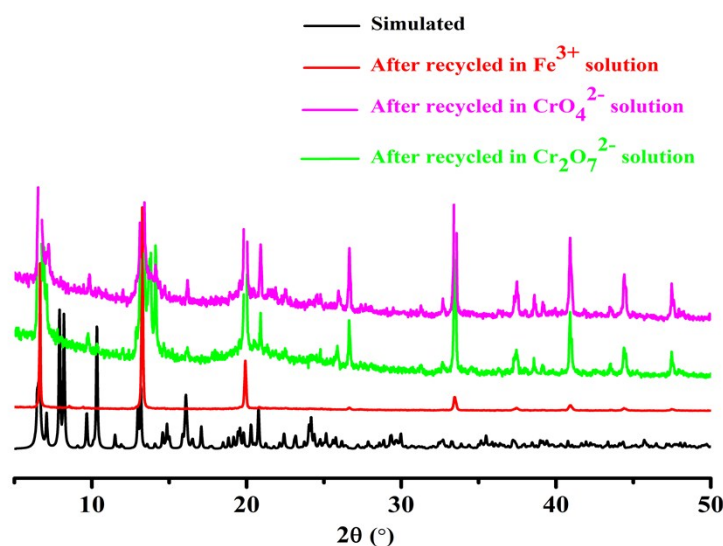


Fig. S11 The PXRD patterns of **1** treated by Fe^{3+} , CrO_4^{2-} and $\text{Cr}_2\text{O}_7^{2-}$ aqueous solutions.

Sample	Concentration of Cd ²⁺ (ug/mL)
Blank sample (H ₂ O)	0.0196
Initial solution after immersing in H ₂ O	0.0228
Final solution after recycle sensing experiment for Fe ³⁺	0.0212
Final solution after recycle sensing experiment for CrO ₄ ²⁻	0.0201
Final solution after recycle sensing experiment for Cr ₂ O ₇ ²⁻	0.0199

Fig. S12 ICP experiments of **1** after immersing in different solution.

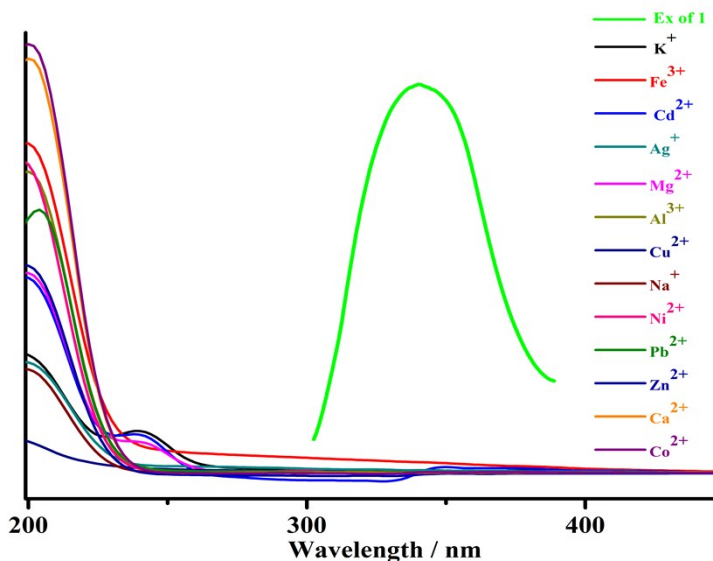


Fig. S13 UV-Vis adsorption spectrum of M(NO₃)_n aqueous solution and the excitation spectrum of **1**.

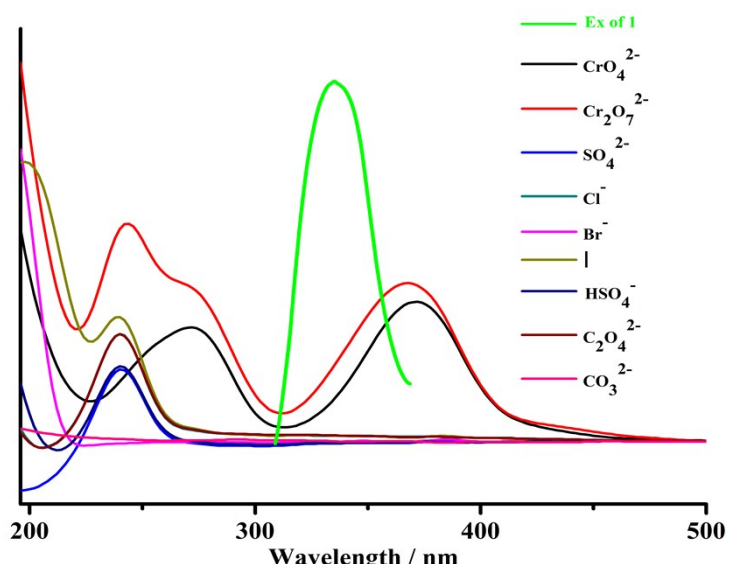


Fig. S14 UV-Vis adsorption spectrum of K_n(A) aqueous solution and the excitation spectrum of **1**.

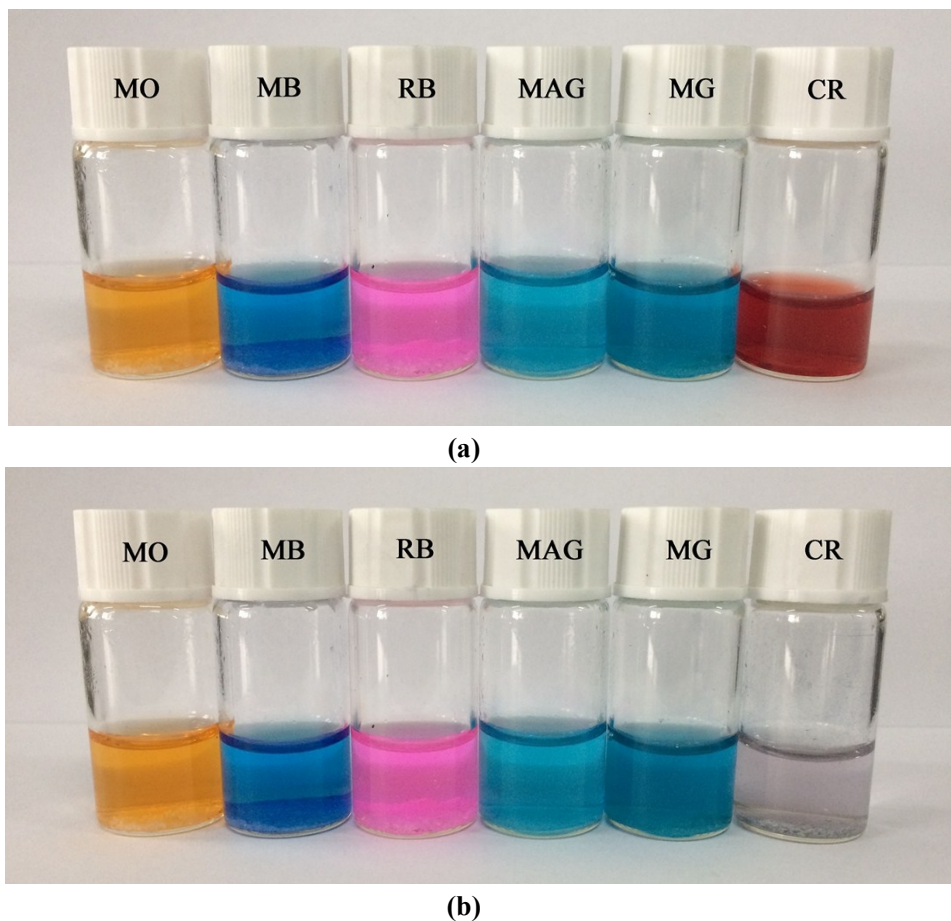


Fig. S15 Selective adsorption of CR with addition of **1** before (a) and after (b).

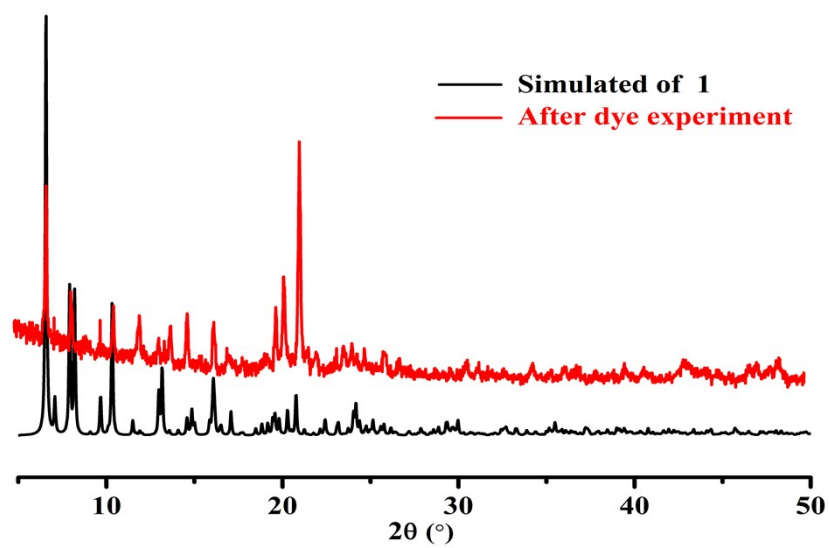


Fig. S16 PXRD powder diffraction patterns of **1** after dye experiment.